WPHCD-PR(18) 19949

M Thumm et al.

Design Studies and Analysis of Operational Limits of 0.24-THz Gyrotrons for DEMO

Preprint of Paper to be submitted for publication in
Chinese Journal of Terahertz Science and Technology

This work has been carried out within the framework of the EUROfusion Consortium and has received funding from the Euratom research and training programme 2014-2018 under grant agreement No 633053. The views and opinions expressed herein do not necessarily reflect those of the European Commission.

Design Studies and Analysis of Operational Limits of 0.24-THz Gyrotrons for DEMO

M. Thumm [1,2*], K. A. Avramidis [1], J. Franck [1], G. Gantenbein [1], S. Illy [1], J. Jin [1], P. C. Kalaria [1], I. Gr. Pagonakis [1], S. Ruess [1,2], C. Wu [1] and J. Jelonnek [1,2]

Karlsruhe Institute of Technology (KIT), Kaiserstr. 12, 76131 Karlsruhe, Germany

[1] Institute for Pulsed Power and Microwave Technology (IHM)

[2] Institute of High Frequency Techniques and Electronics (IHE)

[*] Email: manfred.thumm@kit.edu

Abstract: Electron Cyclotron Heating and Current Drive (ECH&CD) systems using gyrotrons as RF sources play a key role in present controlled thermonuclear fusion plasma experiments and are also planned for the future European DEMOnstration power plant (DEMO). Following the development of 1 MW continuous wave (CW) 140 GHz and 170 GHz gyrotrons for the W7-X stellarator and the ITER tokamak, respectively, the conceptual designs of tubes with frequencies up to approximately 270 GHz are ongoing at KIT. Along with a 237.5 GHz, 2 MW coaxial-cavity gyrotron design, a 236 GHz, 1 MW hollow-cavity approach is under investigation, as backup solution. In both cases, operating modes have been selected considering multi-frequency operation at around 170 GHz, 204 GHz, 237 GHz and 270 GHz for multi-purpose applications and fast-frequency tunability in steps of 2-3 GHz within the frequency range of ±10 GHz around the operating center frequency for plasma stability control.

At 237.5 GHz, a coaxial-cavity design for the $TE_{49,29}$-mode (eigenvalue ~ 158) has been found and optimized using realistic electron beam parameters with quite promising 1.9 MW output power and 33 % interaction efficiency at a maximum cavity wall loading of 2 kW/cm². At 203.8 GHz, oscillating in the $TE_{42,25}$-mode (eigenvalue ~ 136), the same cavity could deliver 1.9 MW output power with 32 % interaction efficiency at reduced maximum cavity wall loading of 1.7 kW/cm². For 170 GHz operation in the $TE_{35,21}$-mode (eigenvalue ~ 113), the corresponding parameters would be 1.8 MW, 31 % and 1.3 kW/cm².

In the case of a $TE_{43,15}$-mode (eigenvalue ~ 103) hollow-cavity gyrotron operating at 236.1 GHz, again considering realistic electron beam parameters in the cavity (rms velocity spread: 6 %, radial width: $\lambda/4$) and a realistic conductivity of the anticipated cavity material Glidcop, the results suggest stable output power of 0.92 MW with an interaction efficiency of 36 % at a maximum cavity wall loading of 2 kW/cm². For the $TE_{37,13}$-mode (eigenvalue ~ 89) at 203.0 GHz and the $TE_{31,11}$-mode (eigenvalue ~ 74) at 170.0 GHz the corresponding values are 1.15 MW and 1.55 MW and 35% and 33%, respectively, at the same wall loading.

The development of magnetron injection guns (MIGs) with high electron beam quality and of multi-stage depressed collectors (MDCs) for energy recovery is necessary to achieve the required total gyrotron efficiency of > 60 %.

Keywords: DEMO, electron cyclotron heating and current drive (ECH&CD), multi-frequency gyrotrons, frequency step-tunable gyrotrons, coaxial-cavity gyrotrons, mode selection, high-order modes, magnetron injection gun, quasi-optical mode converter, broadband synthetic diamond Brewster and tunable windows.

1. Introduction

From the technological point of view, Electron Cyclotron Heating (ECH) is considered to be a mature auxiliary heating method for ITER, due to the availability of 1 MW continuous-wave (CW) 170-GHz gyrotrons and to the simplicity of wave launching and wave-plasma coupling. However, Electron Cyclotron Current Drive (ECCD) alone is not sufficient for long-pulse

discharges in ITER because of the lower CD efficiency compared to ion cyclotron CD, lower hybrid CD and neutral beam CD. This is evident since the 170 GHz EC H&CD system of ITER has not been designed with the main goal of maximizing the amount of CD efficiency [1]. Conversely, the EC H&CD system of a future, commercially attractive tokamak DEMOnstration fusion reactor operating under stationary conditions must be optimized to provide the maximum possible CD efficiency. The achievable ECCD efficiency in two DEMO scenarios has been investigated in [2], one for pulsed and one for steady state operation. Millimeter (mm)-wave beam propagation, absorption and current drive have been simulated by using beam-tracing techniques and including momentum conservation in electron-electron collisions. For mid-plane wave launching the achievable CD efficiency has been found to be limited by 2nd harmonic absorption. Higher efficiencies can be obtained by injecting the millimeter (mm)-wave beams from the top of the tokamak, using wave absorption by more energetic, less collisional electrons. CD efficiencies competitive with those usually achieved by neutral beam CD have been calculated. Assuming the EUROfusion 2012 baseline for DEMO with aspect ratio $A = R/a$ (major/minor plasma radius) of 4.0 and $B > 7$ T the operation frequencies for optimum CD are significantly above 200 GHz, while lower frequencies around 170 GHz and 200 GHz appear useful for plasma start-up and bulk heating. However, in the meantime DEMO machines with smaller aspect ratio are being discussed [3]. Table 1 summarizes the gyrotron frequencies f required for EC H and EC CD versus the aspect ratio and the magnetic field. Even for $A = 3.1$ frequencies of up to approximately 200 GHz are needed.

Table 1: Gyrotron frequencies f needed for plasma heating and non-inductive current drive for different values of aspect ratio A and toroidal magnetic field B_t (γ is a measure for the current drive efficiency) [3].

$A = R/a$	**2.60**	**3.1**	**3.6**	**4.0**
B_t **[T]**	4.2	5.7	7.0	7.6
f **for Heating**	118	160	197	213
f **for Current Drive**	144	196	240	280
γ **[A/m^{2}MW] (Top Launch)**	0.16	0.32	0.36	0.45

The requirements for DEMO gyrotrons are as follows:

- **Unit power:** Considering the mandatory total heating power for DEMO, gyrotrons with a unit power of 2 MW will be needed. Due to the present technological constraints (maximum heat removal), such high unit power can be provided only by very high-order volume mode coaxial-cavity gyrotrons [4], since Ohmic cavity wall loading scales with $f^{5/2}/[\chi^2(1-C_c^2)]$, where χ is the mode eigenvalue and $C_c = R_c/R_{cav}$ is the relative caustic radius of the mode (R_{cav} and R_c are the cavity and caustic radius, respectively). Furthermore, the longitudinally corrugated inner conductor in coaxial cavities reduces mode competition [4]. The maximum

achievable output power at very high frequencies will be determined by the continuously evolving limitations of the core technologies, such as the maximum thermionic emission for long cathode lifetimes, thermal wall loading of cavity and collector, efficiency of depressed collector and superconducting magnet technology.

- **Multiple frequencies**: Slow frequency tunability (within a few minutes) in leaps of 30 – 40 GHz (termed: multi-frequency operation), where 2 - 4 frequencies are related to the transmission maxima of a plane single-disk Chemical-Vapor-Deposition (CVD) diamond window, is considered advantageous for multi-purpose use of fusion gyrotrons, e.g. for a steady-state or a pulsed DEMO reactor or for upgrades of the ITER- and Wendelstein 7-X (W7-X) ECH systems. Two-frequency gyrotrons (140 GHz and 105 GHz) are operating at ASDEX Upgrade [5].
- **Step-wise frequency tunability**: For plasma stabilization employing simple fixed antenna systems fast frequency step-tunability in 2-3 GHz steps within the maximum frequency span of +/- 10 GHz during the pulse is required (within a few seconds) [6]. Such tubes need broadband or tunable CVD-diamond output windows [7-13].
- **Output beam quality**: > 95 %. The mode purity demonstrated for ITER and W7-X gyrotrons is 97 - 98 % [14-17].
- **Reliability**: > 99 %. The 170 GHz ITER gyrotrons demonstrate 95 % (Japan and Russia) [14] and the 140 GHz W7-X gyrotrons (Europe) show 98 % [16,17].
- **Efficiency**: Minimum 60 %. Excellent quality of the electron beam, excellent alignment of the tube components and magnetic field and the use of a multi-stage depressed collector (MSDC) are needed to fulfill this requirement.

Physical design studies towards DEMO compatible gyrotrons, including cavity, magnetron injection gun (MIG), quasi-optical output coupler and MDC, are being performed at the Karlsruhe Institute of Technology (KIT). A coaxial gyrotron cavity design for the $TE_{49,29}$ mode (co-rotating with the beam electrons) at 237.5 GHz has been developed and optimized. The corresponding mode series with good multi-frequency properties is:

$$TE_{35,21}\,(170\ \text{GHz}) - TE_{42,25}\,(203.8\ \text{GHz}) - TE_{49,29}\,(237.5\ \text{GHz}) - TE_{56,33}\,(271.3\ \text{GHz}).$$

The frequency has been chosen such that the allied mode $TE_{35,21}$ matches the ITER frequency of 170 GHz and the highest frequency mode $TE_{56,33}$ at around 271 GHz could be used for EC CD in a high-magnetic field DEMO version. The azimuthal neighboring modes of $TE_{49,29}$ have a frequency separation of 2 GHz and nearly the same radial location of the field maximum which is required for fast frequency tuning for plasma stabilization. The present paper describes the simulation results for the three lower modes of this series and the design of cavity and MIG.

As an alternative, more conservative backup solution, design considerations for a hollow-cavity 1 MW gyrotron have been performed, based on a corresponding series of modes:

$$TE_{31,11}\,(170\ \text{GHz}) - TE_{37,13}\,(203\ \text{GHz}) - TE_{43,15}\,(236.1\ \text{GHz}) - TE_{49,17}\,(269.1\ \text{GHz}).$$

In this case the first two modes at 170 GHz and 203 GHz and the allied modes $TE_{25,9}$ at 137 GHz and $TE_{19,7}$ at 104 GHz have already been successfully experimentally tested by the QST gyrotron team in Japan [18].

In both cases of coaxial and hollow-cavity gyrotron (cavity radius R_{cav}) proper operation of the internal quasi-optical launcher (with radius R_L) and optimum coupling of the hollow electron beam to the operating cavity TE_{mn} mode (with eigenvalue χ_{mn}) can only be achieved when the relative caustic radii $C_c = m/\chi_{mn}$ and thus the absolute caustic radii R_c of the cavity modes are almost the same. Then also the Brillouin angles $\theta_B = \arccos[1 - (R_{cav}/R_L)^2]^{1/2}$, the azimuthal output radiation spread angles $2\phi = 2\arccos(C_c)$ at the launcher cut and the required cut lengths $L = 2\pi R_L \sin\phi /(\phi \tan\theta_B)$ of the cavity modes at different frequencies are almost the same.

2. Design of a 2 MW coaxial-cavity gyrotron

KIT has finished the pre-design for a 2 MW coaxial-cavity gyrotron, which can operate with good performance at 237.5 GHz. The $TE_{49,29}$ cavity mode is the result of a careful mode-selection strategy considering quasi-optical output coupler and CVD diamond output window [19,20], allowing the modes $TE_{35,21}$ (170 GHz) and $TE_{42,25}$ (203.8 GHz) as further operating modes (see Fig. 1). The priority of these initial studies was the optimization of the cavity [21] and of the triode-type magnetron injection gun (MIG) [22] for multi-frequency operation with respect to the $TE_{49,29}$ main design mode.

In the following, we present the imposed technical design restrictions, realistic assumptions for the electron emission and corresponding simulation results for all three operating modes. For interaction and MIG simulations, the European proprietary codes SELFT [23], EURIDICE [24], and ARIADNE [25], ESRAY [26] were used, respectively.

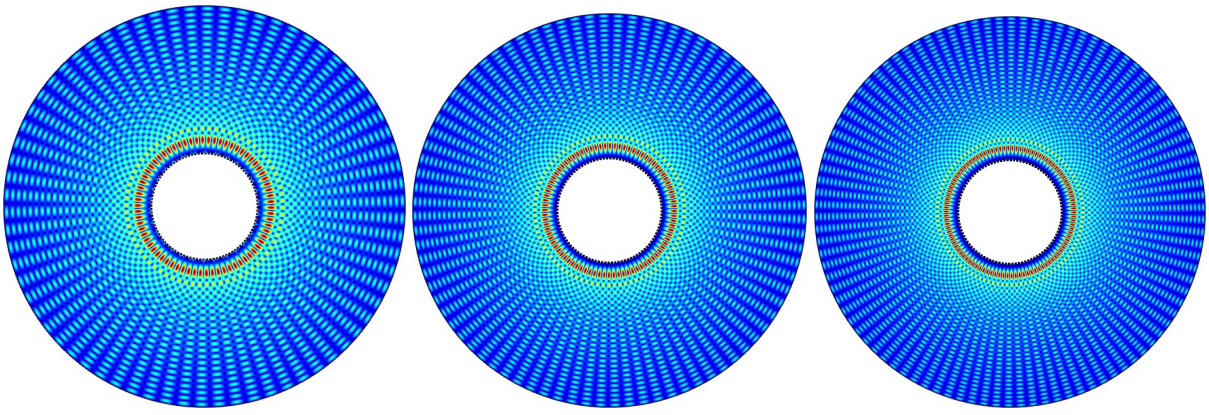

Fig. 1 Transversal intensity profiles of the non-rotating modes $TE_{35,21}$, $TE_{42,25}$ and $TE_{49,29}$.

Table 2 summarizes the features of the chosen cavity mode series with 1.856 mm thickness of the CVD-diamond window disk (- 20 dB reflection bandwidth = 2.2 GHz). The maximum deviation of the relative caustic radii C_c is 0.26 %, which leads to a maximum horizontal shift of

the mm-wave output beam from the window center in the order of only 50 μm [27] and thus allows to use the same beam matching optics for all the different cavity modes. Table 3 shows the cavity mode spectrum for frequency tunable operation in 2 GHz steps over an 18 GHz bandwidth around the center mode. Here the maximum deviation of C_c is 2.5 % resulting in a maximum horizontal beam shift of the order of 2 mm [27, 28].

Table 2 Properties of operating modes of a multi-purpose, multi-frequency coaxial-cavity gyrotron with 1.856 mm thick single-disk CVD-diamond vacuum window together with possible fusion plasma applications (UG: Upgrade, H: Heating, CD: Current Drive) [28]. The corresponding DEMO aspect ratio is given in brackets.

Frequency [GHz] Application	170.00 ITER UG H	203.75 ITER UG CD DEMO CD (3.1) DEMO H (3.6)	237.50 DEMO H (4.0) DEMO CD (3.6)	271.25 DEMO CD (4.0)
Cavity Mode	$TE_{35,21}$	$TE_{42,25}$	$TE_{49,29}$	$TE_{56,33}$
Bessel Zero	113.1329	135.5957	158.0584	180.5209
Relative Caustic Radius C_c	0.3094	0.3097	0.3100	0.3102
Normalized Window Thickness [λ]	5/2	6/2	7/2	8/2
Window Center Frequency [GHz]	169.64	203.57	237.50	271.43

Table 3 Properties of operating modes of a frequency step-tunable coaxial-cavity gyrotron with broadband or tunable CVD-diamond vacuum window [28]. Frequency band: 228.6 GHz < f < 246.4 GHz. Frequency steps: Δf = 2 GHz.

Freq. [GHz]	228.6	230.6	232.5	233.5	235.5	237.5	239.5	241.5	242.5	244.5	246.4
Δf [GHz]	2.0	2.0	1.0	2.0	2.0		2.0	2.0	1.0	2.0	2.0
Cavity Mode	$TE_{47,28}$	$TE_{48,28}$	$TE_{49,28}$	$TE_{47,29}$	$TE_{48,29}$	$TE_{49,29}$	$TE_{50,29}$	$TE_{51,29}$	$TE_{49,30}$	$TE_{50,30}$	$TE_{51,30}$
C_c	0.309	0.313	0.317	0.302	0.306	0.310	0.314	0.317	0.304	0.307	0.311

2.1. Design assumptions

In this study, the maximum current density of the temperature limited Tungsten dispenser cathode emitter of the magnetron injection gun (MIG) was taken as 4 A/cm^2. With an emitter radius of 65 mm, a slant angle of 25° and an emitter width of 4.3 mm (3.9 mm width projected to the gyrotron axis), an electron beam current of 70 A can be achieved. The pitch factor α (ratio of perpendicular and parallel velocity component) of the electrons has been assumed to be around

1.25. The electron beam energy for $TE_{49,29}$-mode operation is limited by the allowed maximum Ohmic loading on the cavity walls (2.0 kW/cm^2 at the outer wall and 0.2 kW/cm^2 on the coaxial insert) and was taken as the upper boundary for all three operating modes. For $TE_{49,29}$-mode operation and with an appropriate MIG design (see Fig. 2), one obtains an rms spread in the perpendicular electron velocity component ($\delta_{\beta,perp}$) of around 1 % at the cavity entrance, which has no significant influence on the interaction efficiency [29]. However, additional spread has to be considered from emitter surface roughness [30] and from possible non-uniform emission (non-uniform heating or non-uniform work-function distribution). In $TE_{49,29}$-mode operation, a typical emitter rms surface roughness of 2 µm leads to an increase of $\delta_{\beta,perp}$ to 3.4 %. For interaction calculations, $\delta_{\beta,perp}$ = 6 % was assumed, which means that less than 3 % spread may result from azimuthal variations of cathode work function and heating temperature. These beam parameters allow generation of 1.9 MW mm-wave power at 33 % electronic efficiency.

The triode-type MIG (with modulation anode), which can be made more compact than a diode-type version, has been designed such that reflection and trapping of secondary electrons [31] is avoided for all three operating modes and the depth of potential wells has been kept small in order to avoid Penning discharges. Despite its relative compactness, the electric field within the MIG nowhere exceeds 7 kV/mm on its metallic surfaces. An initial design for a 10.5 T magnet with 270 mm warm bore-hole diameter, supplied by an industrial manufacturer, has been used for the simulations.

The considered cavity has a radius of 31.78 mm and a length of 15 mm (straight middle section, including parabolic smoothening sections). The conical coaxial insert in this region has 100 longitudinal impedance corrugations (each having a width and depth of 0.3 mm) and a radius

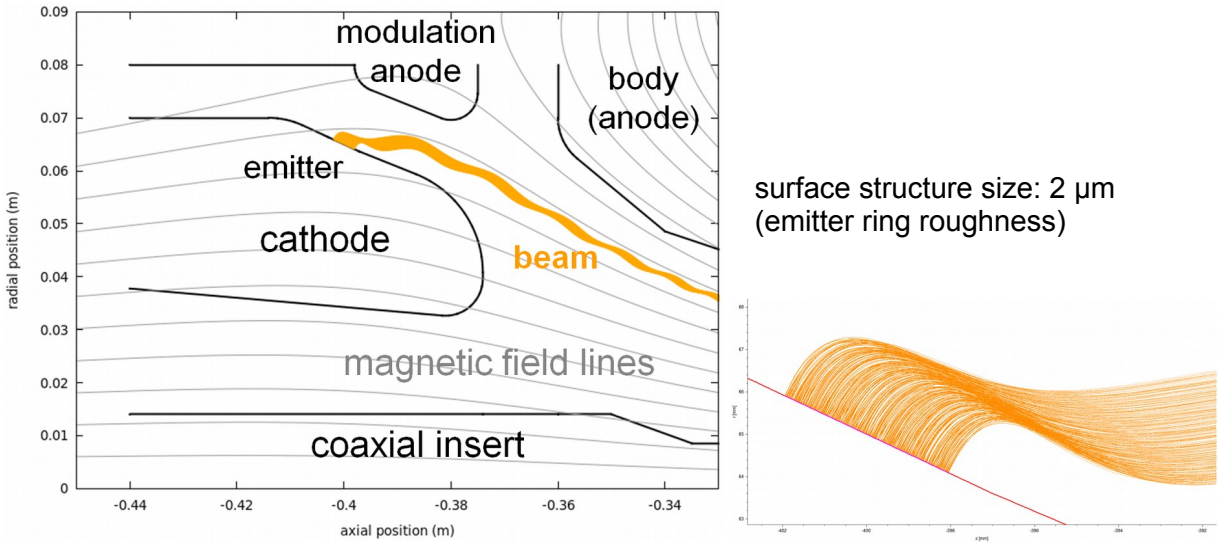

Fig. 2 Design of the triode-type MIG for the coaxial cavity-gyrotron with laminar electron beam, including magnetic field lines and the electron beam for operation in the $TE_{49,29}$ mode at 237.5 GHz [29].

between 8.66 mm (cavity entrance) and 8.4 mm (cavity exit). The diffractive quality factor is Q_{diff} = 2700. Calculations on the influence of misalignment of the coaxial insert revealed a

required precision of 150 μm in order to keep mode competition and conversion sufficiently low.

2.2. Design results

Table 4 summarizes the operating parameters and simulation results for the three frequencies under consideration. These values have been found using self-consistent time-dependent start-up simulations with at least ten modes each, taking into account the full guiding center distribution, velocity spread and voltage depression of the electron beam (see Fig. 3 for the $TE_{49,29}$-mode start-up employing 74 modes). While the optimum electron beam radius in the cavity is almost constant and likewise is the overall magnetic field profile, the modulation anode voltage has to be varied significantly to compensate the different magnetic field strengths at the emitter in order to obtain a similar pitch factor around 1.25.

Due to its own space-charge, the electron beam experiences a voltage depression between emitter and cavity. However, it is well known that, compared to a conventional hollow gyrotron cavity, this depression is significantly reduced by the coaxial insert [4]. As one can see from Table 4, the voltage depression is only around 2 kV for all three operating modes.

The Ohmic loading of the corrugated coaxial insert for the various operating modes should be considered carefully. While the outer cavity wall loading increases with increasing operating frequency at otherwise comparable operating parameters, the loading on the insert decreases. This is due to the broader mode maximum for lower-order modes at lower frequencies [29].

Table 4 Operating parameters of the three operating coaxial-cavity modes [29].

Window thickness in multiples of λ/2	5	6	7
Operating cavity mode	**$TE_{35,21}$**	**$TE_{42,25}$**	**$TE_{49,29}$**
Cavity mode eigenvalue	113.1329	135.5957	158.0584
Oscillation frequency [GHz]	**170.00**	**203.75**	**237.50**
Magnetic field at emitter [T]	0.137	0.165	0.191
Electron accelerating voltage [kV]	85.6	87.9	87.4
Modulation anode voltage [kV]	53.7	46.6	37.5
Electron beam current [A]	69.4	70.0	69.3
Velocity spread by MIG [%]	6.8	4.3	3.4
Magnetic field in cavity [T]	6.82	8.22	9.58
Electron beam energy [keV]	83.4	86.0	85.6
Perp. RMS velocity spread [%]	6.8	4.3	3.4
Guiding center radius at cavity [mm]	10.28	10.27	10.24
Pitch factor at cavity	1.27	1.25	1.22
λ-to-beam-thickness ratio (in cavity)	6.2	5.1	4.4
Output power [MW]	**1.78**	**1.90**	**1.90**
Electronic interaction efficiency [%]	**31**	**32**	**33**
Peak outer cavity wall loading [kW/cm²]	1.3	1.7	2.0
Peak coaxial insert loading [kW/cm²]	0.5	0.3	0.2

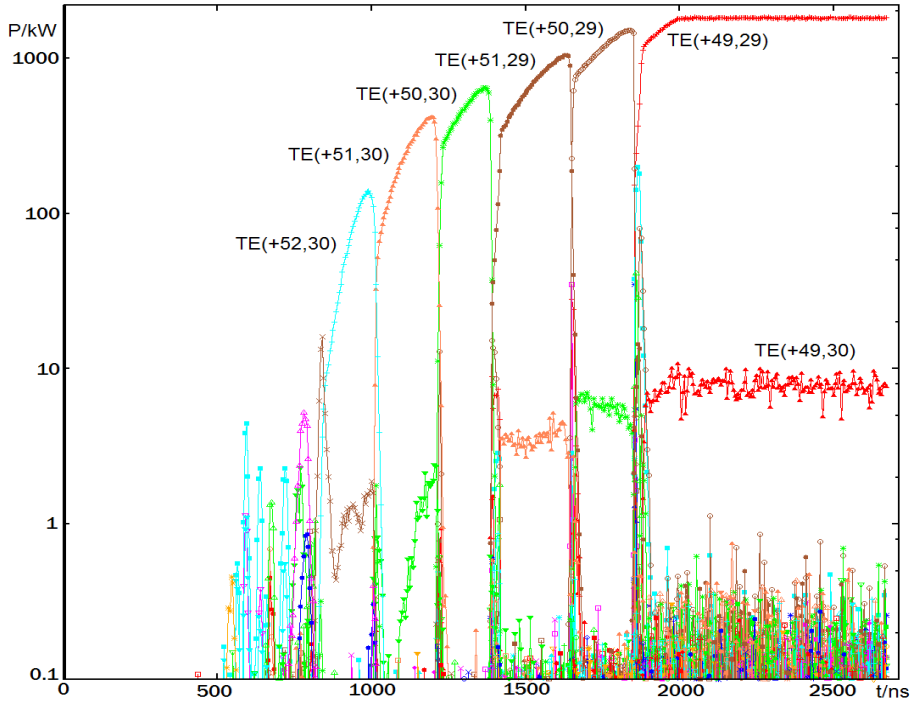

Fig. 3 Startup scenario simulation for operation in the $TE_{49,29}$ mode at 237.5 GHz. 74 competing modes have been considered. Voltages have been ramped up linearly, with beam current following according to the Schottky effect. At t = 2000 ns simulation time, the ramp-up was stopped as the design values were reached [29]. Modes co-rotating with the electrons are marked by a plus sign, counter-rotating modes by a minus sign.

3. Design of a 1 MW hollow-cavity gyrotron

In order to provide an alternative, more conservative backup design, studies on a corresponding hollow-cavity gyrotron have been performed at KIT employing the mode selection approach for high-frequency, high-power DEMO gyrotrons described in [20] where considerations of multi-frequency operation of the tube are included [28].

3.1. Modes for multi-frequency operation

Based on this study, the selected operating frequencies and their corresponding applications for different aspect ratios of DEMO are listed in Table 5 along with the selected modes for the multi-frequency operation [3]. Initially, the operating modes for 170 GHz and 203 GHz were suggested and successfully tested by the QST gyrotron team in Japan [18, 32]. We have extended this mode series for the higher frequencies and suggest suitable modes for 236 GHz and 269 GHz. The relative caustic radii of all modes are nearly the same with only a small deviation of 0.08 % from the average value. Consequently, the suggested mode series has a high rating in the scheme discussed in [19].

Table 5 Properties of the selected operating modes of a multi-frequency hollow cavity gyrotron with 1.861 mm thick single disk CVD-diamond vacuum window.
(H = plasma heating, CD = current drive, A = DEMO aspect ratio)

Window transmission band (-20 dB reflection) [GHz]	168.2-170.4	202.0-204.2	235.8-238.1	269.7-271.9
Applications	H (A=3.1)	H (A=3.6) CD (A=3.1)	H (A=4.0) CD (A=3.6)	CD (A=4.0)
Cavity mode	$TE_{-31,11}$	$TE_{-37,13}$	$TE_{-43,15}$	$TE_{-49,17}$
Mode eigenvalue	74.32	88.76	103.21	117.65
Relative caustic radius	0.4171	0.4168	0.4166	0.4165
Normalized window thickness	5/2	6/2	7/2	8/2

3.2 Modes for frequency-step tunability

Brewster-angle windows have a very broad transmission bandwidth and their use is essential to achieve frequency-step tunability. The design and development of Brewster windows is ongoing for high-power, long-pulse gyrotrons [32]; however, otherwise tunable window systems could also be used for frequency step-tuning. The proposed mode series for frequency-step tunability is shown in Table 6. These suitable modes around 236 GHz and over a 20 GHz bandwidth in steps of 2-3 GHz have a maximum relative caustic radius deviation of 3.5 % from the average value. All modes have the same rotation since they will all use the same quasi-optical system. The detailed mode selection approach and step-frequency tunability of a 236 GHz DEMO gyrotron has been discussed in [19]. With a proper superconducting magnet design, it should be possible to achieve both multi-frequency operation and fast frequency-step tunability for a given tube.

Table 6 Suitable operating modes and their properties for a frequency-step tunable, hollow cavity gyrotron. Frequency steps: Δf = 2 - 3 GHz.

Frequency [GHz]	227.4	230.3	233.1	236.1	238.9	241.8	243.9
Δf [GHz]	2.9	2.8	3.0	0	2.8	2.9	2.1
Cavity mode	$TE_{-40,15}$	$TE_{-41,15}$	$TE_{-42,15}$	$TE_{-43,15}$	$TE_{-44,15}$	$TE_{-45,15}$	$TE_{-43,16}$
Relative caustic radius	0.402	0.407	0.412	0.417	0.421	0.427	0.403

After successful selection of the main operating mode $TE_{43,15}$ at 236.1 GHz, the physical design has been finalized [34,35].

3.3 Cavity design

The geometry of the optimized hollow cavity is shown in Fig. 4. It is a cylindrical-symmetric structure with a straight midsection, a down-taper section and an up-taper section. To reduce unwanted mode conversion due to abrupt discontinuities, adjacent sections are connected via

parabolic smoothing. The calculated cavity radius for the $TE_{-43,15}$ mode at 236 GHz is 20.88 mm and the electron beam radius for maximum coupling is 9.06 mm. As per the current technological possibilities, a maximum wall loading of 2 kW/cm^2 has been considered for the cavity design. The midsection length L_2 is a major factor of the cavity performance. Our parametric analysis of L_2 is presented in Fig. 5. A reasonable value of $\alpha = 1.25$ was assumed. After this investigation, $L_2 = 12$ mm was selected for further analysis, which is a good compromise between the demands for high output power, high efficiency and acceptable mode competition. Finally, the cavity taper angles and parabolic smoothing sections have been chosen to be $\theta_1 = 2.5°$, $\theta_3 = 2.0°$, $D_1 = 4$ mm and $D_2 = 5$ mm, respectively ($L_1 = L_3 = 16$ mm). In this case the Ohmic quality factor (Q_{ohm}) and the diffractive quality factor (Q_{diff}) is 62937 and 1443, respectively. As one can see from Table 7, the midsection length L_2 has the largest impact on gyrotron performance. This justifies that it was the first parameter to address during the design procedure.

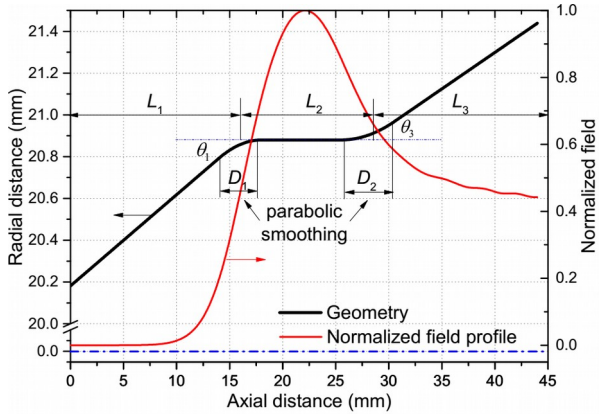

Fig. 4 Geometry of the conventional design for a DEMO gyrotron cavity with the longitudinal field profile of the operating mode [34].

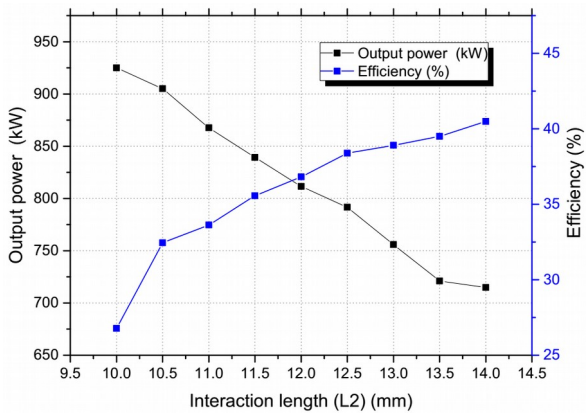

Fig. 5 Output power and efficiency of cavity with various interaction section lengths (L_2) from 10 mm to 14 mm [34].

Table 7 Influence of the individual geometrical parameters on the overall cavity performance [34].

Parameter	L_2	θ_1 and θ_2	D_1 and D_2	L_1 and L_3
Investigated range	10 – 15 mm	1 – 4º	1 – 4 mm	10 – 19 mm
Output power variation	25.6 %	17.7 %	14 %	3.7 %
Efficiency variation	40.7 %	16.7 %	12 %	4 %

3.4 Cavity performance

The detailed RF behavior of the proposed cavity is investigated to validate the physical design and find the most suitable operating parameters of the gyrotron. As discussed in Section 3.2, the mode $TE_{+43,15}$ (eigenvalue ≈ 103.2132) was selected as the operating mode at 236 GHz. As it is of high order, its spectrum is quite dense, therefore it is especially important to identify start-up conditions and operating parameters to excite this mode with good stability margin. The simulations were done using the in-house code packages CAVITY [23] and EURIDICE [24].

Figure 3: Geometry of the conventional design for a DEMO gyrotron cavity with the longitudinal field profile of the operating mode.

Initially, the operating point for the final cavity design was defined by single-mode simulations. The main selection criteria for the operation parameters were: more than 35 % interaction efficiency, high output power and stable RF output. For optimum operation, an axial magnetic field of 9.165 T at the cavity center is required. Since a magnet system for a DEMO gyrotron is currently under investigation and yet to be finalized, a uniform magnetic field along the cavity was considered for the analysis. Electron beam current and beam electron energy are 43 A and 61 keV, respectively, assuming a pitch factor $\alpha = 1.25$. Instead of the conservative electrical conductivity of $\sigma = 1.4\times10^7$ S/m, an updated value of $\sigma = 1.9\times10^7$ S/m was used for the Glidcop cavity wall which includes the temperature dependence of the skin depth and the measured wall roughness [34].

As a next step, multi-mode, time-dependent, self-consistent simulations were performed to study the influence of the neighboring modes on the main mode operation. For a rigorous analysis, 99 possibly relevant modes were considered for the start-up simulation. The beam energy was raised from 20 keV to 61 keV linearly in the start-up phase, while the pitch factor varied adiabatically and the beam current varied according to the temperature-limited regime of a diode-type magnetron injection gun (MIG). The parameters were kept constant at their nominal values to check the stability of the operating point. In Fig. 6, the start-up scenario considering an ideal electron beam (e.g. no velocity spread or radial width) is presented, as simulated by EURIDICE. Stable RF output of 960 kW with an interaction efficiency of 38 % has been achieved. As in usual gyrotron start-ups, modes having a high relative coupling (more than 0.8) and an operating frequency close to the design frequency (236 GHz) are excited during start-up (time variable from 0 to 3000 in arbitrary unit).

Due to practical limitations of a MIG, it is not possible to generate an ideal electron beam without velocity spread and radial width. Therefore, it is important to check cavity performance with an electron beam with velocity spread and radial width, henceforth termed realistic beam. For the cavity design presented here, the individual effects of velocity spread and radial width on the gyrotron performance are discussed in detail in [34]. The result for a realistic electron beam (6% perpendicular velocity spread, λ/4 radial width) is presented in Fig. 7. In this case, stable RF-output has also been achieved, but with slightly lower output power of 920 kW and interaction efficiency of 36 %. During the simulation, the output power of all considered neighboring modes at the operating point remains at less than 0.1 % of the operating mode power, which itself remains constant. This result indicates stable operation without spurious mode generation or mode loss.

It is desirable to have stable main mode operation within a certain range of the operating parameters. This will further ensure robust operation during actual experiments. In Fig. 8a, the stability of the operation is shown with respect to the beam electron energy. The energy has been

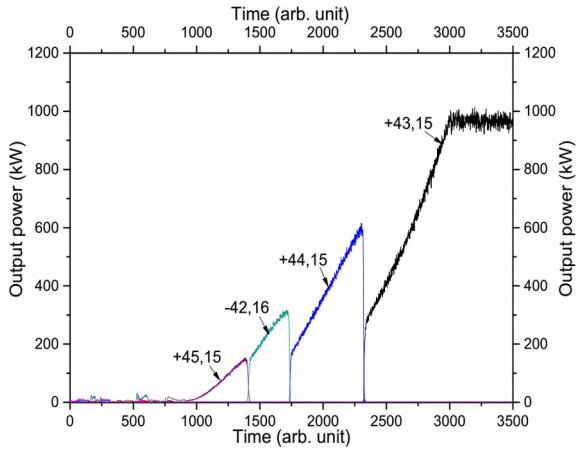

Fig. 6 Start-up scenario considering 99 neighboring modes and an ideal electron beam [34].

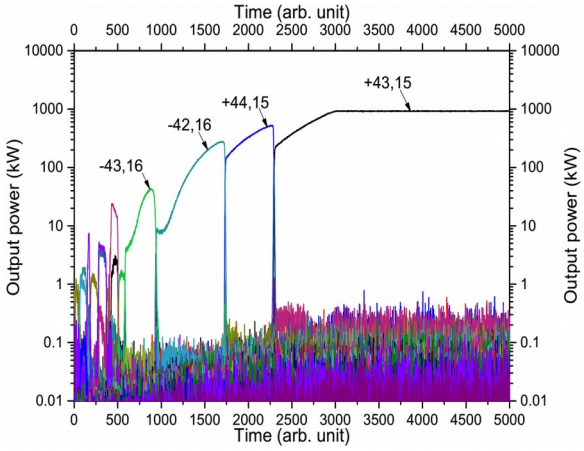

Fig. 7 Start-up scenario for longer time duration, and with the realistic electron beam parameters. Beam energy linearly increases from 20 keV to 61 keV till t=3000 and remains constant till t=5000 (arb. unit) [34].

increased in steps of 0.1 keV from 61 keV until mode loss. From single-mode and multi-mode time-domain analyses by EURIDICE, it was verified that mode loss is only due the detuning and not because of mode competition [34]. With the suggested magnetic field of 9.165 T, the operating mode is stable up to the electron beam energy of 62.3 keV, i.e. there is a 1.3 keV margin with respect to the nominal beam energy. The stability margin of the tube operation can be extended by operating the gyrotron at higher magnetic field, which corresponds to lower detuning. Using a modified magnetic field of 9.177 T at the cavity center, a stability margin of up to 2 keV can be achieved. This, of course, comes at the expense of power and efficiency at the operating point, which are now reduced by 900 kW and 35 %, respectively (see Fig. 8b).

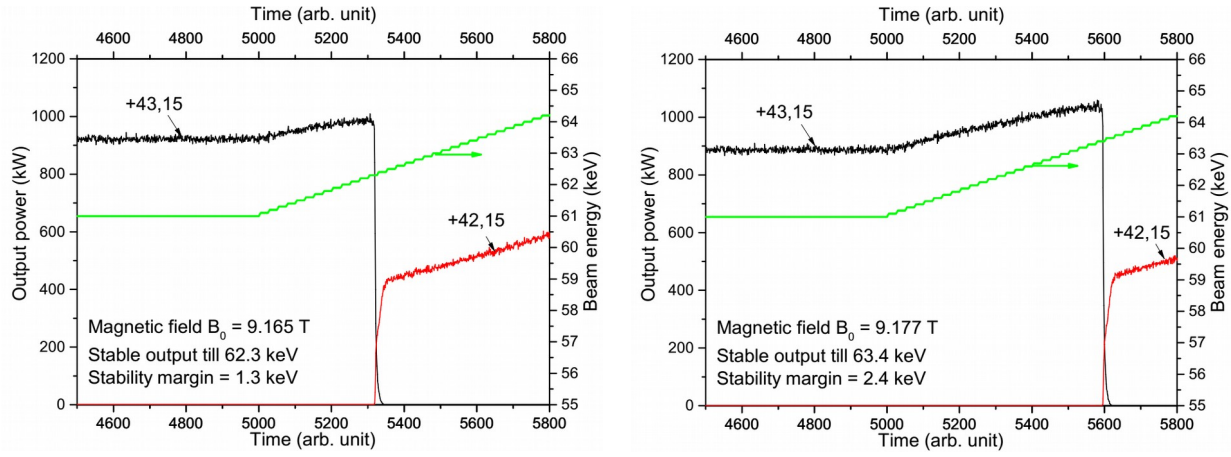

(a) (b)

Fig. 8 Stability analysis of the operating point. The beam energy has been increased in 0.1 keV steps (a) with magnetic field of 9.165 T, (b) 9.177 T [34].

As discussed in Section 3.3, the cavity wall-loading is a major limiting factor for the output power of the DEMO gyrotron. If the ohmic loading limit of 2 kW/cm^2 is relaxed (i.e. if a more efficient cooling would be used) than more power could be possible. This is illustrated in Table 8, where the operating parameters, output power and efficiency for the same cavity geometry and with ideal beam parameters, but with higher wall loading are listed. The result confirms the approximate proportionality between output power and peak wall loading and motivates possible improvements of the cavity cooling capabilities.

Table 8 Operating parameters and output power of 236 GHz gyrotron with higher cavity wall loading [34].

Maximum wall loading (kW/cm^2)	Beam energy (keV)	Beam current (A)	Output power (kW)	Interaction efficiency (%)
2.00	61	43	960	38
2.18	65	45	1070	38
2.43	65	50	1200	38

Multi-frequency, multi-purpose operation of the proposed cavity design has been also validated with realistic multi-mode simulations like those presented above. The operating parameters were optimized for all four suggested frequencies of 170 GHz/ 203 GHz/ 236 GHz and 269 GHz. The results are summarized in Table 9.

Table 9 Multi-frequency operation of the proposed hollow cavity DEMO gyrotron. The frequency dependence of Glidcop conductivity is included [34].

Frequency (GHz)	**170.0**	**203.0**	**236.1**	**269.1**
Mode	$TE_{-31,11}$	$TE_{-37,13}$	$TE_{-43,15}$	$TE_{-49,17}$
Mode eigenvalue	74.325	88.769	103.213	117.656
Magnetic field [T]	6.785	7.975	9.165	10.349
Beam radius [mm]	9.13	9.10	9.06	9.04
Beam electron energy [keV]	81	70	61	55
Beam current [A]	59	48	43	38
Diffractive quality factor Q_{diff}	820	1171	1443	1839
Ohmic Wall loading [kW/cm^2]	2.00	1.99	2.00	1.99
Effective conductivity [10^7 S/m]	2.12	2.01	1.91	1.82
Without electron velocity spread and with zero radial electron beam width				
Output power [kW]	**1650**	**1220**	**960**	**821**
Interaction efficiency [%]	**35**	**37**	**38**	**40**
With 6 % velocity spread and λ/4 radial electron beam width				
Output power [kW]	**1550**	**1150**	**920**	**765**
Interaction efficiency [%]	**33**	**35**	**36**	**38**

3.5 Step-wise frequency tuning

The possibility of fast frequency step-tunability of the cylindrical cavity DEMO gyrotron has been verified theoretically with the help of time-dependent self-consistent multi-mode simulations [35]. The upper two plots of Fig. 9 show the variation of magnetic field and beam energy over the time, respectively, and the lower two plots show the efficiency and output power of the excited mode with consideration of the large number of neighboring modes. The beam energy has been modified at every stage to maintain optimized detuning for sufficiently high efficiency and output power. It is clear from the result that the operating frequency can be easily varied by modifying the magnetic field. Stable RF output of around 1 MW can be achieved at the various decreasing operating frequencies in a continuous run. The speed of the frequency tuning is mainly dependent on the rate of the change of magnetic field.

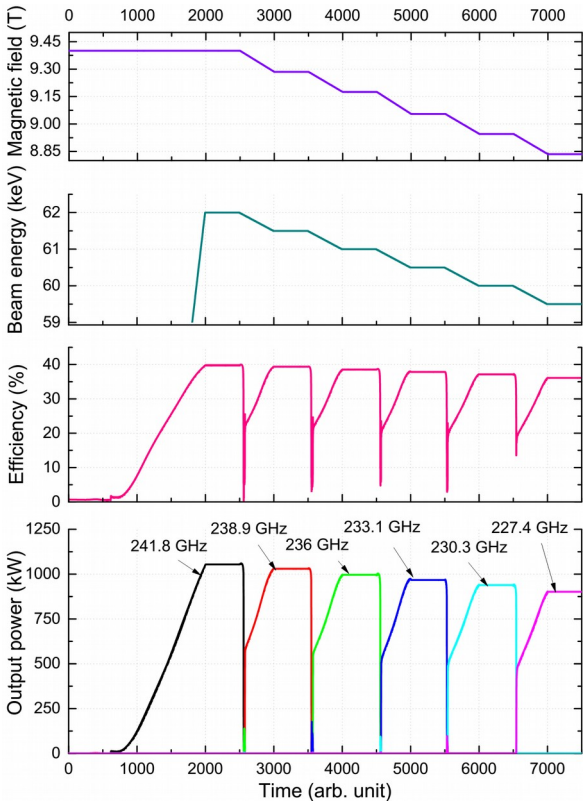

Fig. 9 Step-wise fast-frequency tuning from high to low frequency with changing magnetic field and beam energy. Stable output power (~ 1 MW) with an interaction efficiency of more than 36 % has been achieved at the different operating frequencies [35].

Unlike the step-frequency tuning from high frequency to low frequency, it is not possible to achieve frequency tunability at the desired 2-3 GHz steps from low frequency to high frequency by simply increasing the magnetic field, due to hysteresis effects [35]. This case has been studied considering frequency step-tunability from the 236 GHz $TE_{43,15}$ mode to the 238.9 GHz $TE_{44,15}$ mode. The optimum magnetic field for the excitation of the modes $TE_{43,15}$ and $TE_{44,15}$ with high efficiency is 9.175 T and 9.285 T, respectively. In the case of multi-mode time-dependent

simulations, when the magnetic field (B_0) has been increased from 9.175 T to 9.285 T, the $TE_{43,15}$ mode remained excited with low detuning and low output power. Since the cavity is the same for all suggested frequencies, a possible solution is to reduce the beam energy to a low level until the working mode is detuned and then excite the desired mode at the higher frequency by increasing the beam energy again and adjust the magnetic field accordingly (see Fig. 10).

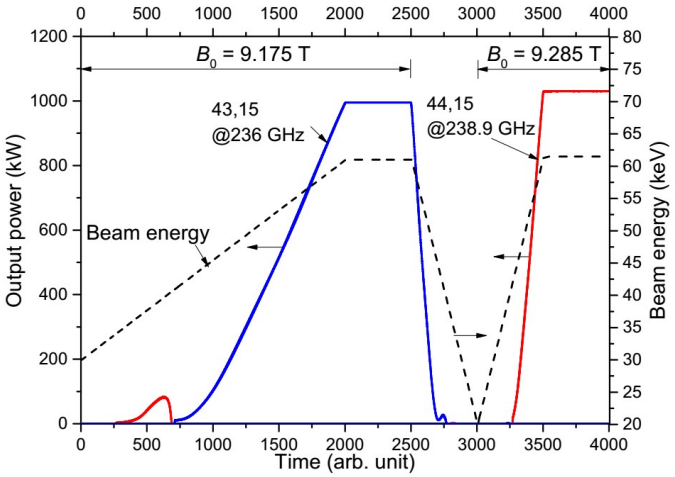

Fig. 10 Frequency step-tuning from low to high frequency by controlling beam energy and magnetic field [35].

The KIT in-house code for launcher analysis and synthesis ("TWLDO") [36] was used for the design of the launcher of the quasi-optical output coupler. The input radius is 22.37 mm (corresponding to $1.07 \cdot R_{cav}$), launcher length and cut length are 227.11 mm and 60 mm, respectively. As the relative caustic radii of all the modes selected for step-frequency tunability are close to each other, the performance of the launcher is nearly identical for all the different operating modes at the various frequencies. The simulated Fundamental Gaussian Mode Content (FGMC) for the different frequencies is listed in Table 10. Using the commercial 3-D full-wave code SURF3D, the radiation pattern of the launcher has been calculated for all frequencies at a radial distance of 60 mm. Compared to the field profile at the frequency of 236 GHz, the RF beam is slightly shifted for the other frequencies due to the small difference in their relative caustic radii, but the overall beam profile remains Gaussian-like with more than 92 % of FGMC.

Table 10 Fundamental Gaussian Mode Content (FGMC) of the designed launcher for different operating frequencies of the step-frequency tunable gyrotron [35].

Frequency [GHz]	227.4	230.3	233.1	236.0	238.9	241.8	243.9
Cavity TE mode (indices m,n)	40,15	41,15	42,15	43,15	44,15	45,15	43,16
Relative caustic radius	0.402	0.407	0.412	0.417	0.421	0.427	0.403
FGMC (%)	93.11	95.42	96.67	97.31	97.02	95.88	92.35

4. Multi-stage depressed collector

One major possibility to improve the total efficiency of a gyrotron above 60 % is to use a multi-stage depressed collector (MDC). That technology is well known from highly efficient traveling wave tubes (TWT) for space applications [37]. Those collectors use electrostatic lens and repulsion forces to separate electrons with different energies of the spent electron beam in several intermediate steps of the depression voltage along the electron beam axis. In case of gyrotron operation there are also two known theoretical MDC concepts: one is unwinding the magnetic field non-adiabatically to a weak magnitude [38]; the other is using the $\boldsymbol{E} \times \boldsymbol{B}$ drift of the electrons [39]. Even though several considerations about MSDC designs for gyrotrons exist in the literature, there is not any successful implementation of that technology in an experimental gyrotron.

In the frame of EUROfusion at KIT, the MSDC technology shall be pushed significantly forward. Initial steps towards new, experimentally feasible $\boldsymbol{E} \times \boldsymbol{B}$ drift MSDC design concepts have already been undertaken at KIT [40-42].

5. Conclusions

DEMO-compatible multi-frequency high-power gyrotrons with the main operating frequency in the range of 200 to 240 GHz are under development at KIT in the framework of the EUROfusion Consortium. Time-dependent, self-consistent multi-mode interaction simulations have been performed, including realistic electron beam velocity spread and beam width. The permitted maximum Ohmic loading of the cavity wall was limited to 2 kW/cm^2.

Coaxial-cavity tubes can generate stable 1.9 MW mm-wave power in CW operation at 33 % electronic efficiency (without depressed collector) in the main cavity mode $TE_{49,29}$ at 237.5 GHz. Multi-frequency behavior has been investigated. While the triode-type magnetron injection gun design for the three chosen operating modes $TE_{49,29}$ at 237.5 GHz, $TE_{42,25}$ at 203.8 GHz and $TE_{35,21}$ at 170.0 GHz is promising, the Ohmic loading of the coaxial insert increases for operation at the lower frequencies.

As an alternative backup approach, conceptual design studies on a corresponding hollow-cavity 1-MW-class gyrotron have also been undertaken. Here, the main cavity mode is $TE_{43,15}$ at 236.1 GHz and the lower frequency modes are $TE_{37,13}$ at 203.0 GHz and $TE_{31,11}$ at 170.0 GHz. Operation at 269.1 GHz in the $TE_{49,17}$ mode also has been studied. Almost 1 MW CW output power at 236.1 GHz can be achieved with an electronic efficiency of 36 % (without depressed collector). For plasma stabilization employing simple fixed antenna systems, the feasibility of fast frequency step-tunability (within a few seconds) in 2-3 GHz steps with a maximum span of +/- 10 GHz has been investigated.

The development of multi-stage depressed gyrotron collectors for efficient energy recovery is under progress at KIT in order to achieve the required total gyrotron efficiency of above 60 %.

Acknowledgments

This work has been carried out within the framework of the EUROfusion Consortium and has received funding from the Euratom research and training programme 2014-2018 under grant agreement No. 633053. The views and opinions expressed herein do not necessarily reflect those of the European Commission.

Parts of the simulations presented in this work have been carried out using the HELIOS super-computer at IFERC-CSC and the Marconi-Fusion supercomputer facility.

The authors are glad to acknowledge very helpful discussions with Minh Quang Tran from EPFL-SPC in Lausanne, Switzerland.

References

[1] T. Imai, N. Kobayashi, R. Temkin, et al.. "ITER R&D: auxiliary systems: electron cyclotron heating and current drive system", *Fusion Eng. and Design*, 55, 281-289 (2001).

[2] E. Poli, G. Tardini, H. Zohm, et al.. "Electron-cyclotron-current-drive efficiency in DEMO plasmas", *Nuclear Fusion*, 53, 013011 (10 pp) (2013).

[3] G. Granucci, G. Aiello, S. Alberti, et al.. "Conceptual design of the DEMO EC-system: main developments and R&D achievements", *Nuclear Fusion*, 57, 116009 (8pp) (2017).

[4] B. Piosczyk, G. Dammertz, O. Dumbrajs, et al.. "A 2-MW, 170-GHz coaxial cavity gyrotron", *IEEE Trans. on Plasma Science*, 32, 413-417 (2004).

[5] D. Wagner, J. Stober, F. Leuterer, et al.. "Status, operation and upgrade of thr ECRH system at ASDEX Upgrade", *J. of Infrared, Millimeter, and Terahertz Waves*, 37, 45-54 (2016).

[6] H. Zohm and M. Thumm, "On the use of step-tuneable gyrotrons in ITER", *J. of Phyics.: Conf. Series*, 25, 274-282 (2005).

[7] O. Braz, G. Dammertz, M. Kuntze and M. Thumm, "D-band frequency step-tuning of a 1 MW gyrotron using a Brewster output window", *Int. J. of Infrared and Millimeter Waves*, 18, 1465-1477 (1997).

[8] M. Thumm, "Development of output windows for high-power long-pulse gyrotrons and EC wave applications", *Int. J. of Infrared and Millimeter Waves*, 19, 3-14 (1998).

[9] B. Piosczyk, A. Arnold, G. Dammertz, et al.. "Step-frequency operation of a coaxial cavity gyrotron from 134 to 169.5 GHz", *IEEE Trans. on Plasma Science*, 28, 918-923 (2000).

[10] M. Thumm, A. Arnold, E. Borie et al.. "Frequency step-tunable (114-170 GHz) megawatt gyrotrons for plasma physics applications", *Fusion Eng. and Design*, 53, 407-421 (2001).

[11] V.E. Zapevalov, A.A. Bogdashov, G.G. Denisov, et al.. "Development of a prototype of a 1-MW 105-156-GHz multifrequency gyrotron", *Radiophysics and Quantum Electronics*, 47, 396-404 (2004).

[12] I.V. Kazansky, A.V. Kruglov, S.A. Malygin, et al.. "Step-tunable experimental gyrotrons at 75 GHz and 140 GHz ranges", *Proc. 7th Int. Workshop on Strong Microwaves: Sources and Applications*, Nizhny Novgorod, 2008, Vol. 1, 100-102 (2009).

[13] A.G. Litvak, G.G. Denisov, V.E. Myasnikov, et al.. "Recent development resulrs in Russia of megawatt power gyrotrons for plasma installations", *EPJ Web of Conferences*, 32, 04003 (5pp) (2012).

[14] G. G. Denisov, A. G. Litvak, A.V. Chirkov, et al.. "Development status of gyrotron setup for ITER ECW system", *40th International Conference on Infrared, Millimeter, and Terahertz Waves (IRMMW-THz 2015)*, Hong Kong, 2015, H1E-6.

[15] T. Rzesnicki, F. Albajar, S. Alberti, et al.. "Experimental verification of the European 1 MW, 170 GHz industrial CW prototype gyrotron for ITER", *Fusion Eng. And Design*, 123, 490-494 (2017)

[16] G. Gantenbein, V. Erckmann, S. Illy, et al.. "140 GHz, 1 MW CW gyrotron development for fusion applications – Progress and recent results", *J. of Infrared, Millimeter, and Terahertz Waves*, 32, 320-328 (2011).

[17] R.C. Wolf, A. Ali, A. Alonso, et al.. "Major results from the first plasma campaign of the Wendelstein 7-X stellarator", *Nuclear Fusion*, 57, 102020 (13pp) (2017).

[18] Y. Oda, K. Kajiwara, K. Takahashi, et al.. "Development of dual frequency gyrotron and high power test of EC componants", *EPJ Web of Conferences*, 32, 04004 (8pp) (2012).

[19] J. Franck, K. A. Avramidis, G. Gantenbein, et al.. "A generic mode selection strategy for high-order mode gyrotrons operating at multiple frequencies", *Nuclear Fusion*, 55, 013005 (2015).

[20] M. Thumm, J. Franck, P.C. Kalaria, et al.. "Towards a 0.24-THz, 1-to-2-MW-class gyrotron for DEMO", *Terahertz Science and Technology*, 8, No. 3, 85-100 (2015).

[21] J. Franck, S. Illy, K Avramidis, et al.. "Mode selection and resonator design for DEMO gyrotrons", *Proc. 15th IEEE Int. Conf. on Vacuum Electronics (IVEC 2014)*, Monterey, CA, USA, 31-32 (2014).

[22] J. Franck, I. Gr. Pagonakis, K. A. Avramidis, et al.. "Magnetron injection gun for a 238 GHz 2 MW coaxial-cavity gyrotron", *9th German Microwave Conference*, Nuremberg, Germany, Talk S15.2 (2015).

[23] S. Kern, "Numerical Codes for interaction calculations in gyrotron cavities at FZK", *Proc. 21st Int. Conf. Infrared and Millimeter Waves (IRMMW 1996)*, Berlin, Germany, Invited Paper AF2 (1996).

[24] K. A. Avramidis, I. Gr. Pagonakis, C. T. Iatrou, and J. L. Vomvoridis, "EURIDICE: A code-package for gyrotron interaction simulations and cavity design", *EPJ Web of Conferences*, 32, 04016 (2012).

[25] I. Gr. Pagonakis and J. L. Vomvoridis. "The self-consistent 3D trajectory code ARIADNE for gyrotron beam tunnel simulation". *Conf. Digest 29th IRMMW-THz*, Karlsruhe, Germany, 657-658 (2004).

[26] S. Illy, J. Zhang, and J. Jelonnek, "Gyrotron electron gun and collector simulation with the ESRAY beam optics code", *Proc. 16th IEEE Int. Conf. on Vacuum Electronics (IVEC 2015)*, Beijing, China, Talk P1.1 (2015).

[27] O. Prinz, A. Arnold, G. Gantenbein, et al.. "Highly efficient quasi-optical mode converter for a multifrequency high-power gyrotron", *IEEE Trans. on Electron Devices*, 56, 828-834 (2009).

[28] M. Thumm, J. Franck, S. Illy, et al.. "Towards a High-Power Millimeter-Wave Gyrotron for DEMO" *Proc. 5th Int. Workshop on Far-Infrared Technologies (FIRT 2014)*, Fukui, Japan, 5-16, (2014)..

[29] J. Franck, K.A. Avramidis, I.Gr. Pagonakis, et al.. "Multi-frequency design of a 2 MW coaxial-cavity DEMO gyrotron", *Proc. 40th Int. Conf. on Infrared, Millimeter, and Terahertz Waves (IRMMW-THz 2015)*, Hong Kong, Paper MS-16 (2015).

[30] J. Zhang, S. Illy, I.Gr. Pagonakis, et al.. ”Influence of emitter surface roughness on high power fusion gyrotron operation”, *Nuclear Fusion*, 56, 026002 (7pp) (2016).

[31] I.Gr. Pagonakis, B. Piosczyk, J. Zhang, et al.. ”Electron trapping mechanisms in magnetron injection guns”, *Physics of Plasmas*, 23, 023105 (11pp) (2016).

[32] R. Ikeda, R., Y. Oda, T. Kobayashi, et al.. ”Multi-frequency, MW-power triode gyrotron having a uniform directional beam”, *J. of Infrared, Millimeter, and Terahertz Waves*, 38, 531-537 (2017).

[33] G. Gantenbein, A. Samartsev, G. Aiello, et al.. “First operation of a step-frequency tunable 1 MW gyrotron with a diamond Brewster angle output window”, *IEEE Trans. on Electron Devices*, 61, 1806-1811 (2014).

[34] P.C. Kalaria, K.A. Avramidis, J. Franck, et al.. ”Systematic cavity design approach for a multi-frequency gyrotron for DEMO and study of its RF behavior”, *Physics of Plasmas*, 23, 092503 (9pp) (2016).

[35] P.C. Kalaria, K.A. Avramidis, J. Franck, et al.. ”RF behavior and launcher design for a fast frequency step-tunable 236 GHz gyrotron for DEMO”, *Frequenz*, 71, No. 3-4, 161-172 (2017).

[36] J. Jin, M. Thumm, B. Piosczyk, et al.. ”Novel numerical method for the analysis and synthesis of the fields in highly oversized waveguide mode converters”, *IEEE Trans. on Microwave Theory and Techniques*, 57, 1661-1668 (2009).

[37] G. Faillon, G. Kornfeld, E. Bosch, and M. Thumm. “Microwave Tubes”, in “Vacuum Electronics – Components and Devices”, eds. J.A. Eichmeier and M. Thumm, Springer, Berlin Heidelberg New York, 1-84 (2008).

[38] R.L. Ives, A. Singh, M. Mizuhara, et al.. “Design of a multistage depressed collector system for 1-MW CW gyrotrons-Part II: System consideration”, *IEEE Trans. on Plasma Science,* 27, 503-511 (1999).

[39] I.Gr. Pagonakis, J.-P. Hogge, S. Alberti, et al.. “A new concept for the collection of an electron beam configured by an externally applied axial magnetic field”, *IEEE Trans. on Plasma Science,* 36, 469-480 (2008).

[40] I.Gr. Pagonakis, C. Wu, S. Illy, et al.. “Multistage depressed collector conceptual design for thin magnetically confined electron beams”, *Physics of Plasmas*, 23, 43114 (11pp) (2016).

[41] C. Wu, I.Gr. Pagonakis, G. Gantenbein, et al.. ”Conceptual designs of ExB multistage depressed collectors for gyrotron”, *Physics of Plasmas*, 24, 043102 (8pp) (2017).

[42] C. Wu, I.Gr. Pagonakis, S. Illy, et al.. ”Comparison between controlled non-adiabatic and ExB concepts for gyrotron multistage depressed collectors”, *EPJ Web of Conferences*, 149, 04005 (2pp) (2017).